Risk-aware Emergency Landing Planning for Gliding Aircraft Model in Urban Environments

Jakub Sláma Jáchym Herynek Jan Faigl

***Abstract*— An in-flight loss of thrust poses a risk to the aircraft, its passengers, and people on the ground. When a loss of thrust happens, the (auto)pilot is forced to perform an emergency landing, possibly toward one of the reachable airports. If none of the airports is reachable, the aircraft is forced to land at another location, which can be risky in urban environments. In this work, we present a generalization of the previous work on planning safe emergency landing in the case of in-flight loss of thrust such that the risk induced by the loss of thrust can be assessed if none of the airports are reachable. The proposed method relies on planning space discretization and efficient risk propagation through the risk map. The approach can find the least risky landing site and corresponding forced landing trajectory for any configuration in the planning space. The method has been empirically evaluated in a realistic urban scenario. The results support its suitability for risk-aware planning of an emergency landing in the case of in-flight loss of thrust.**

I. Introduction

Urban Air Mobility (UAM) is a trend in modern aviation, standing for personal air transportation on short to medium distances [1]. An increasing number of small aircraft flying in an urban environment can be thus expected in the near future [2] that would put high demands on safety, enabling operation in areas currently forbidden for regular air traffic. Regarding safety, the aviation industry nowadays can be considered safe and modern aircraft reliable due to the high standards and regulations. Still, flying over vulnerable areas, such as urban areas, is restricted to limit possible damage on the ground in a case of an in-flight failure. Further restrictions on flyable areas are not sustainable for the upcoming UAM, as the aircraft are expected to fly over densely populated areas. However, the required increase in reliability is not possible by physical redundancy because it is not economically sustainable. Therefore, minimizing the risk and possible consequences caused by plausible in-flight failure needs to be addressed by other means, such as risk-aware trajectory planning.

A powerplant failure was the leading mechanical cause of non-commercial aircraft accidents in the U.S. in 2014 [3]. According to the report, approximately 80 % of all fatal accidents involved a loss of thrust failure caused by various problems, such as mechanical failure, fuel exhaustion, and bird strike. Furthermore, an engine failure rate of 13 failures per 10^5 flight hours has been recorded in Australia between 2009 and 2014 [4]. Luckily, not all engine failure-related incidents lead to an accident, as an emergency landing may be possible for the in-flight engine failure of US Airways Flight 1549 in 2009. After a complete loss of thrust caused by a flock of birds after take-off from LaGuardia airport, the pilots decided to land at the Hudson river because of insufficient altitude for an emergency landing at any of the nearby airports.

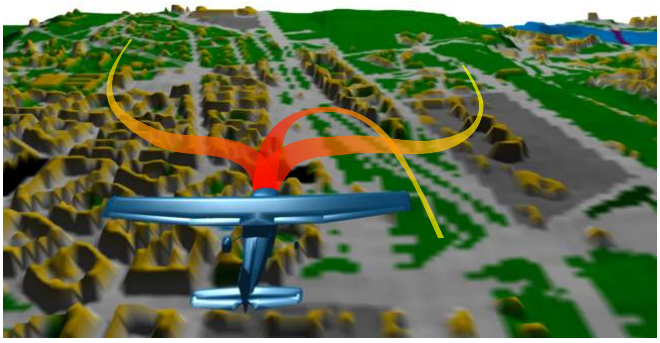

Fig. 1. Visualization of the risk-aware emergency landing problem. If an in-flight loss of thrust happens, an emergency landing must be performed. Landing at an airport can be considered safe; otherwise, the aircraft landing may cause harm to people or properties on the ground. Thus, the goal is to select the most suitable landing site and corresponding emergency landing trajectory to minimize the in-flight loss of thrust-induced risk. Risk evaluation is essential for full risk-aware trajectory planning.

If a safe emergency landing is possible, the risk on the ground can be ranked based on the evaluation ranging from the value of caused damage to the number of casualties [5], [6]. Regardless of the risk definition, trajectory planning plays a critical role in risk mitigation and minimizing the consequences of a possible crash. In our former work on risk-aware trajectory planning [7], we consider a decoupled approach guaranteeing a safe emergency landing for failures with still partially controllable aircraft, such as loss of thrust. The guarantee is based on sufficient altitude allowing an emergency landing, and therefore, the approach restricts aircraft from entering areas from which a successful emergency landing would not be possible.

Although the risk of failures such as loss of thrust is eliminated by guaranteed emergency landing, the restricted areas might be too limiting for considering more failures with the possibility of the emergency landing. Therefore, we propose to address the limitation of the previous approach by determining the least risky emergency landing site for an in-flight loss of thrust failure. Visualized in Fig. 1,

The authors are with the Faculty of Electrical Engineering, Czech Technical University in Prague, Technická 2, 166 27 Prague, Czech Republic. {slamajak|herynjac|faiglj}@fel.cvut.cz

The work has been supported by the Czech Science Foundation (GAČR), projects No. 22-30043S and No. 22-05762S. The support of the Grant Agency of the CTU in Prague under grant No. SGS22/168/OHK3/3T/13 is also gratefully acknowledged. The access to the computational infrastructure of the OP VVV-funded project CZ.02.1.01/0.0/0.0/16_019/0000765 "Research Center for Informatics" is gratefully acknowledged.

the problem consists of the landing site determination and the corresponding emergency landing trajectory planning. The proposed solution builds on the emergency landing planner [8] that is generalized for determining the least risky landing location and planning a suitable corresponding emergency landing. Based on the performed computational evaluation, the proposed solution showed to be feasible and scales with the selected levels of altitude discretization and considered aircraft maneuvers.

The rest of the paper is organized as follows. An overview of the related work is provided in the following section. The formal definition of the studied problem is given in Section III together with considered models of the vehicle motion constraints. The proposed method is presented in Section IV. The performed empirical evaluation results are in Section V. Conclusion and final remarks are in Section VI.

II. Related Work

The studied problem of *Risk-aware Emergency Landing Planning* (RELP) is to determine the most suitable landing sites together with the landing trajectory satisfying motion constraints of the vehicle and considering possible ground risk. There is no single approach addressing all the parts of the studied RELP problem, to the best of the authors' knowledge; therefore, we provide a brief overview of the related approaches in this section.

Dubins Airplane model [9] can be utilized to generate motion maneuvers for a simplified model of aircraft motion constraints. The model extends Dubins vehicle [10] into a 3D environment. It is simplified by allowing abrupt changes in pitch and roll angles within the given limits, as the pitch and roll angles can change significantly faster than the heading angle. Further model modification to fit small fixed-wing aircraft is presented in [11]. A pre-defined discrete set of possible turning radii has been used in [12] as aircraft maneuvers for gliding paths evaluation for the Hudson river accident. In [8], the authors propose the optimization of the turning radii to minimize the altitude loss of a gliding aircraft and thus support safe gliding at the emergency landing site in the case of loss of thrust failure.

If an emergency landing at a safe site is impossible, a landing spot imposing minimal risk to people or properties on the ground must be determined. A risk map for small Unmanned Aerial Vehicles (UAVs) [5] models risk to people, ground vehicles, and other aircraft. However, buildings are omitted due to the minor impact energy of such UAVs.

In [6], the risk is assumed as a probability of three consecutive events: (i) loss of control followed by an uncontrolled crash; (ii) collision with somebody; and (iii) casualty of the hit person. The authors of [13] build a ground risk map based on multiple layers given by population density and sheltering factor provided by buildings, where the ground risk can be determined with respect to (w.r.t) various in-flight malfunctions. A ground risk map based on terrain segmentation is proposed in [14], which is further infused with exact building information and critical infrastructure location assigned one of five pre-defined risk levels. Besides, in the case of an in-flight aircraft disintegration, a stochastic approach for risk determination can be used [15].

Adaptation of human pilots' emergency landing procedures for UAVs is studied in [16]. A method for selecting the most suitable emergency landing site and a corresponding gliding trajectory in the case of loss of thrust is proposed in [8]. The therein proposed method yields maximizing the altitude margin from the terrain as the authors argue that the excess altitude can be lost if needed. However, if an airport is not reachable, an off-airport emergency landing must be performed, and a suitable landing site must be chosen. The roads can be used for an emergency landing site in the case of loss of thrust by small aircraft, and forced landings on public roads are studied [17], [18]. In general, the forced landing is to determine the least risky road segment using data from available databases such as the current traffic.

Possible landing locations can be selected from a continuous ground map using the Maximal Covering Location Problem [19], where the goal is to select locations for a given number of facilities maximizing the coverage of customers. Integer programming can solve the problem; however, greedy heuristics are reported to provide satisfactory solutions [20].

Having a risk map and methods to assess the risk, the risk-aware planners [21], [22] plan a flight path minimizing the induced risk w.r.t multiple failures. The former work [7] eliminates the risk caused by loss of thrust by guaranteeing the existence of a safe emergency landing to one of a set of dedicated landing sites. However, it might be beneficial to determine a risk-aware landing site when an emergency landing at the given sites is not possible. Therefore, we propose determining the least risky location for an emergency landing and finding the gliding trajectory toward it in the case of in-flight loss of thrust.

III. Problem Statement

The *Risk-aware Emergency Landing Planning* (RELP) problem is to find the least risky forced landing trajectory in the case of in-flight loss of thrust. The problem is to determine the most suitable landing location based on the current state of the aircraft, together with the emergency landing trajectory that satisfies the gliding motion constraints of the aircraft. The problem follows the safe emergency landing [8]; however, the necessary background is formally defined in this section to make the paper self-contained.

Planning the trajectory that **satisfies the motion constraints** is addressed by using Dubins Airplane [9] for which the aircraft state is described as $q = (x, y, z, \theta, \psi)$, where $(x, y, z) \in \mathbb{R}^3$ denotes the aircraft position, $\theta \in \mathbb{S}$ stands for its heading angle, and $\psi \in \mathbb{S}$ denotes the aircraft pitch angle. The configuration space is $\mathcal{C} = \mathbb{R}^3 \times \mathbb{S}^2$, and the aircraft state can be described as

$$\begin{bmatrix} \dot{x} \\ \dot{y} \\ \dot{z} \\ \dot{\theta} \end{bmatrix} = v \begin{bmatrix} \cos\theta\cos\psi \\ \sin\theta\cos\psi \\ \sin\psi \\ u_\theta \rho^{-1} \end{bmatrix}. \tag{1}$$

The vehicle forward velocity is denoted v. The heading angle is controlled by the control input $u_\theta \in [-1, 1]$, and the

minimum turning radius is denoted ρ. Dubins Airplane model allows abrupt changes in the pitch angle ψ. Since the pitch angle changes significantly faster than the heading angle θ, the simplification is considered a suitable approximation for small aircraft such as Cessna 172 in the computational evaluation of the proposed planner. However, the pitch angle must be within its limits $\psi \in [\psi_{\min}, \psi_{\max}]$. Obstacles might be present in the environment, and the aircraft trajectory is planned in the collision-free part $\mathcal{C}_{\text{free}}$ of $\mathcal{C}$.

A forced landing imposes a risk to people or property on the ground at the landing location. So, it is necessary to **evaluate the imposed ground risk** for the landing location, which is the main generalization of the addressed RELP problem compared to former work [7], [8]. The risk $\mathcal{R}$ is given by the landing location $\boldsymbol{x}$, impact energy E, and impact angle γ. We follow the risk determination proposed in [13]; the ground risk is given as a probability of casualty in the case of a forced landing at $\boldsymbol{x}$ as

$$\mathcal{R} = p_{\text{hit}}(\boldsymbol{x}, \gamma) p_{\text{casualty}}(\boldsymbol{x}, E)\,, \tag{2}$$

where p_{hit} denotes the probability of hitting a person, and p_{casualty} is the probability of casualty if the person is hit.

The probability p_{hit} is adopted from [13] as

$$p_{\text{hit}}(\boldsymbol{x}, \gamma) = \rho(\boldsymbol{x}) A_{\exp}(\gamma) \tag{3}$$

with $\rho(\boldsymbol{x})$ being the population density at $\boldsymbol{x}$, and $A_{\exp}(\gamma)$ denotes the area exposed to the landing aircraft given as

$$A_{\exp}(\gamma) = 2(r_p + r_{\text{uav}}) \frac{h_p}{\tan(\gamma)} + \pi (r_p + r_{\text{uav}})^2\,, \tag{4}$$

where dimensions of an average person are characterized by the radius r_p and height h_p. The aircraft size is characterized by the radius r_{uav} of the disk-shaped aircraft outline.

The probability p_{casualty} of a hit person is also adopted from [13] as

$$p_{\text{casualty}}(\boldsymbol{x}, E) = \frac{1-k}{1 - 2k + \sqrt{\frac{\alpha}{\beta}} \left(\frac{\beta}{E}\right)^{\frac{3}{S(\boldsymbol{x})}}}\,, \tag{5}$$

where $k = \min\left(1, \left(\frac{\beta}{E}\right)^{\frac{3}{S(\boldsymbol{x})}}\right)$, $S(\boldsymbol{x})$ denotes the sheltering factor at $\boldsymbol{x}$. The value of α is the impact energy needed to achieve $p_{\text{casualty}} = 50\,\%$ when $S(\boldsymbol{x}) = 6$, and β is the impact energy needed for causing a casualty for $S \to 0$. We use $\beta = 34\,\text{J}$ in the present work based on [23].

We can express the ground risk map M, quantifying the risk $\mathcal{R}$ by the forced landing at $\boldsymbol{x}$ with the impact energy E, and impact angle γ, as a projection $M : \mathbb{R}^3 \to \mathbb{R}$ given by

$$\mathcal{R} = M(\boldsymbol{x}, E, \gamma)\,. \tag{6}$$

The problem of finding the least risky landing location and planning emergency landing trajectory stands for **minimization of the induced risk to people on the ground**. Let $\mathcal{T} \subset \mathcal{C}_{\text{free}}$ be a set of all configurations on the terrain surface, and let $\Gamma : [0,1] \to \mathcal{C}_{\text{free}}$ be a gliding trajectory from the initial configuration $q_i \in \mathcal{C}_{\text{free}}$ to the landing configuration $q_f \in \mathcal{T}$ such that $\Gamma(0) = q_i$ and $\Gamma(1) = q_f$. The vertical

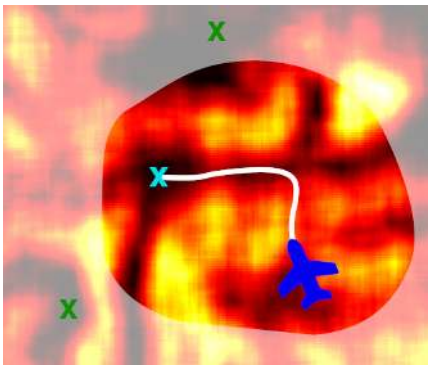

Fig. 2. Visualization of the landing trajectory once the in-flight loss of thrust occurs. Due to losing altitude, the aircraft can reach only the highlighted area, and the nearby airports in green become unreachable. The least risky reachable landing location (in cyan) with an emergency landing trajectory (in white) is determined.

profile of the trajectory Γ has to satisfy the gliding ability of the aircraft, as the only way to maintain the aircraft velocity after the loss of thrust is to lose altitude. Hence, the altitude loss $\mathcal{H}(\Gamma)$ along the trajectory Γ has to be within the limits $\mathcal{H}(\Gamma) \in [\mathcal{H}_{\min}(\Gamma), \mathcal{H}_{\max}(\Gamma)]$. The model of the gliding aircraft is adopted from [8], and the maximum pitch angle needed for maintaining the aircraft velocity is given as

$$\psi_{\max} \approx \sin^{-1}\left(\frac{\rho' S v^2 (C_{\text{D0}} + k H^2}{2W}\right)\,, \tag{7}$$

where ρ' is the air density, S is the wing surface area, C_{D0} is the geometric drag coefficient, k is the lift-induced drag coefficient, $W = mg$ characterizes the aircraft weight m under the gravitational acceleration g, and H is given as

$$H = 2W \sqrt{\left(\frac{v}{Rg}\right)^2 + 1}\,, \tag{8}$$

where R is the turning radius of the aircraft. Note that the roll angle φ is related to the turning radius as

$$\varphi \approx \tan^{-1}\left(\frac{v^2}{Rg}\right)\,. \tag{9}$$

The risk $\mathcal{R}$ induced by the forced landing from the aircraft configuration q and the landing location $q_f \in \mathcal{T}$ is given as

$$\mathcal{R}(q) = M(q_f, E, \gamma)\,, \tag{10}$$

such that there is a gliding trajectory Γ from q to q_f.

The studied planning scenario is visualized in Fig. 2, and the RELP problem stands to determine the least risky landing location for a forced emergency landing in the case of loss of thrust. The problem is formally defined as Problem 3.1, where the least risky landing location is assured by (11). The emergency landing trajectory Γ is required to satisfy the motion constraints (1) and aircraft gliding ability (7).

Problem 3.1 (Risk-aware Trajectory Emergency Landing Planning)

$$\min_{\Gamma, q_f \in \mathcal{T}} \quad M(q_f, E, \gamma) \tag{11}$$

$$\text{s.t.} \qquad \Gamma(0) = q_i,\, \Gamma(1) = q_f \tag{12}$$

IV. Proposed Method

The proposed planner to the introduced RELP problem originates from [8], but using randomized-sampling-based RRT* would be too computationally demanding. Therefore, we propose an explicit sampling of $\mathcal{C}_{\text{free}}$ in a grid manner and planning the emergency landing through pre-calculated possible maneuvers among the grid samples to trade off the computational burden and find a suitable emergency landing trajectory. The planner consists of the risk map determination summarized in Algorithm 1, and emergency landing trajectory extraction summarized in Algorithm 2. The algorithms are detailed in the following paragraphs.

Algorithm 1: Risk Map Creation

Input: $\mathcal{C}_{\text{free}}$ – Collision-free configuration space.
Input: $\mathcal{T}$ – Terrain model.
Parameter: k – Number of heading samples.
Parameter: m – Number of maneuvers.
Parameter: n – Number of nearest nodes.
Parameter: s – Number of forced landing locations.
Parameter: Δd – Horizontal distance between samples.
Parameter: Δz – Vertical distance between samples.
Parameter: $\mathcal{A}$ – Aircraft model.
Output: Risk map G.

1 $Q \leftarrow \texttt{UniformSampling}(\mathcal{C}_{\text{free}}, k, \Delta d, \Delta z)$
2 **for** $q \in Q$ **do**
3 $\quad \mathcal{R}(q) \leftarrow \infty$
4 $\Xi \leftarrow \texttt{SelectLandingSites}(s, \mathcal{T})$
5 $\Lambda \leftarrow \texttt{CreateManeuvers}(\mathcal{A}, k, m, \Delta d, \Delta z)$
6 $G \leftarrow \{\boldsymbol{V} \leftarrow Q \cup \Xi, \boldsymbol{E} \leftarrow \emptyset\}$
7 **for** $\xi \in \Xi$ **do**
8 $\quad Q_{\text{n}} \leftarrow \texttt{Near}(\xi, Q)$
9 $\quad$ **for** $q \in Q_{\text{n}}$ **do**
10 $\quad\quad$ **if** $\texttt{isAdmissible}((q, \xi), \mathcal{T})$ **then**
11 $\quad\quad\quad \mathcal{R}(q) \leftarrow \min(\mathcal{R}(q), \mathcal{R}(\xi))$
12 $\quad\quad\quad q^* \leftarrow \operatorname{argmin}(\mathcal{R}(\texttt{Succesor}(q)), \mathcal{R}(\xi))$
13 $\quad\quad\quad$ **if** $(q, q^*) \notin \boldsymbol{E}$ **then**
14 $\quad\quad\quad\quad \boldsymbol{E} \leftarrow \boldsymbol{E} \setminus (q, \texttt{Succesor}(q)) \cup (q, q^*)$
15 $\quad\quad\quad\quad \texttt{Succesor}(q) \leftarrow q^*$
16 **for** $Q_i \in \texttt{Layers}(Q)$ **do**
17 $\quad$ **for** $q \in Q_i$ **do**
18 $\quad\quad Q_{\text{suc}} \leftarrow \emptyset$
19 $\quad\quad$ **for** $\Gamma \in \Lambda$ **do**
20 $\quad\quad\quad \Gamma \leftarrow \texttt{SetOrigin}(\Gamma, q)$
21 $\quad\quad\quad$ **if** $\texttt{isAdmissible}(\Gamma, \mathcal{T})$ **then**
22 $\quad\quad\quad\quad Q_{\text{suc}} \leftarrow Q_{\text{suc}} \cup \Gamma(1)$ // $\Gamma(1) \in Q$
23 $\quad\quad q_{\text{suc}} \leftarrow \operatorname{argmin}_{q_i \in Q_{\text{suc}}} \mathcal{R}(q_i)$
24 $\quad\quad \mathcal{R}(q) \leftarrow \mathcal{R}(q_{\text{suc}})$
25 $\quad\quad \boldsymbol{E} \leftarrow \boldsymbol{E} \cup (q, q_{\text{suc}})$
26 **return** G

A. Risk Map Construction

In the first step of Algorithm 1, $\mathcal{C}_{\text{free}}$ is uniformly sampled in a grid-like manner by the `UniformSampling` routine. The samples are created within the map limit with the horizontal spacing Δd but with vertical spacing Δz, and k heading samples per each sampled location. A set of samples Q is created with the corresponding risk set to infinity.

Then, a grid-based ground risk map is determined. Since evaluating all possible landing sites is not computationally tractable, only s landing sites from the ground map grid locations are selected by the `SelectLandingSites` method to cover the operational area evenly. The covering follows a greedy heuristic with at least δ distance between landing locations. We assess the risk for each sampled location, and s sites are iteratively selected as the least risk location without the δ vicinity of the already selected locations. In addition to s selected locations, all airports are added (with zero risk) to the set of possible landing sites Ξ.

Since we use a grid-based sampling of $\mathcal{C}_{\text{free}}$, samples $Q_{\text{suc}} \subset Q$ reachable from any $q \in Q$ are located identically w.r.t. the origin sample q, only some connections may not be valid due to terrain and obstacles. Therefore, m generic maneuvers Λ are precomputed by `CreateManeuvers`. The maneuvers must satisfy the gliding ability of the aircraft and connect the origin sample q with the m closest sampled configurations within the grid. Note that the altitude of all reachable samples is lower than the altitude of q as the aircraft glides and has to lose altitude to maintain speed.

Having the landing sites Ξ and maneuvers Λ, the risk-aware landing graph G is iteratively constructed. First, the graph vertices are formed by the samples Q and landing sites Ξ. Then, a set of n closest samples Q_n from which a landing site is reachable is found for each landing site by the `Near` routine. The risk of these samples is set to the risk of the corresponding landing site, and the appropriate edges are inserted into G. If multiple landing sites are reachable from a configuration q, only the least risky one is considered a successor of such a sample. The risk of such a sample is set appropriately as the risk of the least risky reachable landing site (Algorithm 1, Lines 11 to 15).

Finally, the risk propagation in the graph is performed. It can be imagined as a kernel operation in image processing, and it is visualized in Fig. 3. The propagation goes through altitude layers from the bottom to the top. For each sample q, the set of plausible maneuvers Λ is translated such that the maneuvers start at q. Each maneuver is then checked for a collision with the terrain by the `isAdmissible` routine. The endpoints of admissible maneuvers, naturally corresponding to the graph vertices, form a set Q_{suc} of reachable successors of q (Algorithm 1, Lines 18 to 22). Then, the least risky sample $q_{\text{suc}} \in Q_{\text{suc}}$ is determined and selected as the successor of q with the risk set accordingly (Algorithm 1, Lines 23 to 25). Once all layers and all samples from Q are processed, the risk-aware landing graph G is created, and it can be used for assessing a risk associated with any in-flight loss of thrust within the map.

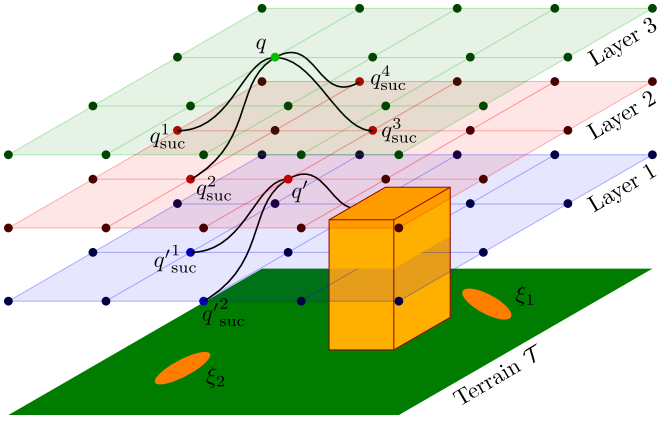

Fig. 3. Visualization of the risk propagation in the graph. The collision-free part of the configuration space $\mathcal{C}_{\text{free}}$ is sampled in a uniform grid-like manner (samples are depicted as small disks), and two landing locations ξ_1 and ξ_2 on the terrain $\mathcal{T}$ are shown as ellipses. The risk is propagated similarly to kernel operations in image processing. Each layer is fully processed before going into the next, higher layer. A set Λ of predetermined maneuvers (black curves) defines a set of reachable nodes q^i_{suc} from the original node q. Due to the identical relative locations within the grid, the set of plausible maneuvers Λ is independent of the original node q. Thus, the same maneuvers can be used for q', except for q'^3_{suc} not being reachable due to collision with an obstacle (in yellow).

B. Extraction of Risk-aware Emergency Landing Trajectory

The risk-aware emergency landing trajectory can be retrieved for any arbitrary configuration q' from the created risk map by the query routine summarized in Algorithm 2. The set Q_n of n closest samples from Q are found by the `Near` routine, and inadmissible connections are discarded. Then, similarly to the expansion process of the risk map construction, the least risky sample q^* from Q_n is selected as the successor of q'. The risk induced by the in-flight loss of thrust at q' is the risk of q^*. The emergency landing path can be extracted by following the successors of the intermediate waypoints until the landing site is reached.

Algorithm 2: Get Emergency Landing Trajectory

Input: q' – Configuration of the loss of thrust event.
Input: G – Risk map.
Input: $\mathcal{T}$ – Terrain model.
Parameter: n – Number of nearest nodes.
Output: Risk $\mathcal{R}(q')$.
Output: Emergency landing trajectory Γ.

Function `GetEmergencyLanding`$(q', G, \mathcal{T})$**:**
  $Q_n \leftarrow$ `Near`(q', G)
  $q^* \leftarrow$ `nothing`
  for $q \in Q_n$ **do**
    if `isAdmissible`$((q', q), \mathcal{T})$ **and** $\mathcal{R}(q) < \mathcal{R}(q^*)$ **then**
      $q^* \leftarrow q$
  $\Gamma \leftarrow (q', q^*)$, $q \leftarrow q^*$
  while $q \notin \Xi$ **do**
    $\Gamma \leftarrow \Gamma \cup (q,$ `Successor`$(q))$
    $q \leftarrow$ `Successor`(q)
  return $\mathcal{R}(q^*)$, Γ

V. Results

The feasibility and suitability of the proposed RELP problem solver have been computationally evaluated in a realistic urban scenario. The performance is further compared with the former approach [8], which, however, does not support the determination of the risk induced by a forced landing at the other-than-airport location. Therefore, the comparison is performed only for the minimum safe altitude required to land successfully at any airport.

The realistic urban scenario is adopted from [7], featuring a 5 km×5 km large mission area over Prague city center. The map is based on OpenStreetMap [24] with terrain profile from [25]. The population density is from [26], and the sheltering factors are adopted from [13]. The aircraft model used is Cessna 172 [8], one of the most used small aircraft.

A risk map is created by the proposed method with the following setup. The configuration space is sampled from the terrain up to 500 m above the lowest terrain point with lateral spacing $\Delta d = 50\,\text{m}$ and vertical spacing $\Delta z = 5\,\text{m}$ between samples. The maneuvers set Λ consists of maneuvers spanning at most six samples in the grid laterally and five samples vertically. The number of the considered heading samples is $k \in [8, 16, 32]$, and the number of the selected landing sites is $s \in [10, 20, 50, 75]$ to examine the scalability of the developed method. The selected landing sites cannot be closer than $\delta = 500\,\text{m}$, and three airports with bi-directional runways are present. Each setup has been run 20 times.

The proposed and reference methods have been implemented in Julia ver. 1.6.2 [27] and executed on a single core of the Intel Xeon Scalable Gold 6146 processor. An example of the resulting forced landings in the case of loss of thrust is depicted in Fig. 4.

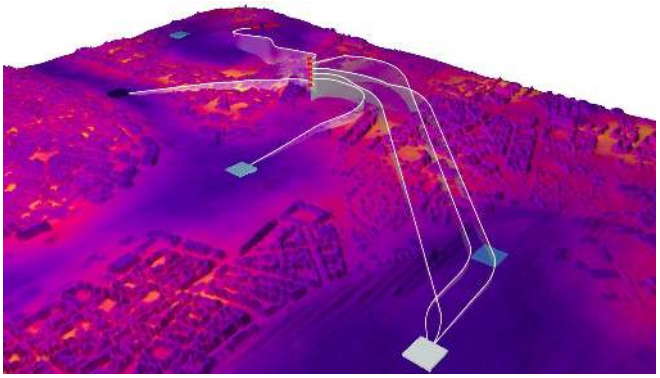

Fig. 4. Visualization of possible forced landings based on the failure altitude. The selected landing sites (squares; the darker, the riskier), possible airport (red rectangle at the top part of the map), and seven failure configurations (in red) at the same location but with varying altitudes are shown; the ground risk is used as terrain overlay. The aircraft is forced to land at the riskiest location at the lowest altitude. Multiple landing sites become reachable with increasing altitudes and landing at the less risky site is possible for higher altitudes. The landing at the airport is preferred once the failure happens at a sufficiently high altitude.

TABLE I

PERFORMANCE CHARACTERIZATION OF THE PROPOSED SOLUTION TO THE RISK-AWARE EMERGENCY LANDING PLANNING (RELP) PROBLEM.

Heading samples k	8				16				32			
Landing sites s	10	20	50	75	10	20	50	75	10	20	50	75
Nodes connected to any landing site [%]	69.5	72.8	76.8	77.7	72.4	75.6	79.1	79.9	72.9	76.1	DNF*	DNF*
Nodes connected to an airport [%]	56.5	56.5	56.5	56.5	59.7	59.7	59.7	59.7	60.3	60.3		
Relative risk [-]	1.30	1.30	1.30	1.30	1.06	1.06	1.06	1.06	1.00	1.00		
Risk $\mathcal{R}(q_1)$ [$\times 10^{-4}$ casualties]	–	–	130.1	130.1	30.0	30.0	30.0	30.0	0.0	0.0	–	–
Risk $\mathcal{R}(q_2)$ [$\times 10^{-4}$ casualties]	45.2	45.2	45.2	45.2	10.6	10.6	10.6	10.6	10.6	10.6	–	–
Risk $\mathcal{R}(q_3)$ [$\times 10^{-4}$ casualties]	–	86.2	86.2	86.2	8.6	8.6	8.6	8.6	8.6	8.6	–	–

*DNF denotes that for the particular problem instance, the solver does not finish within the provided computational time limit of 23 hours.

Results of the computational evaluation are summarized in Table I. The number of landing sites influences the determined nodes with possible landing. Note that nodes without possible landing are near the ground, which is unlikely usable for flying in practice. On the other hand, the number of nodes allowing a safe landing at an airport, and thus with zero risk, does not increase with s. The reachability of airports is given solely by aircraft gliding abilities.

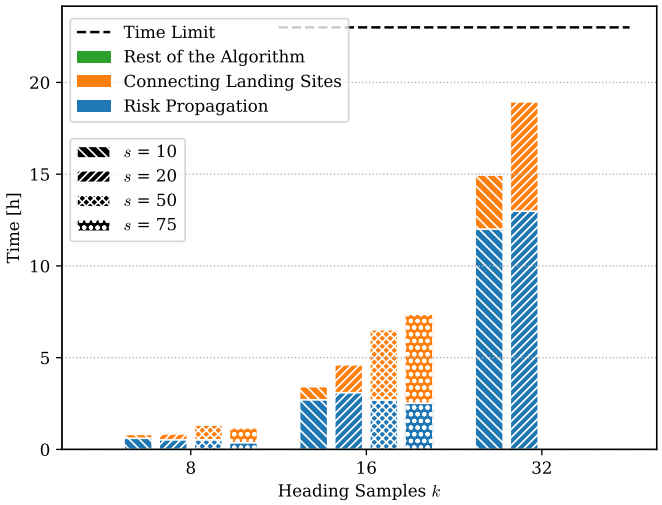

Fig. 5. Required computational time of the proposed method. The time needed for landing site insertion into the risk map increases with the number of inserted landing sites; however, it has a minimal effect on the risk propagation through the map. On the contrary, the number of heading samples influences landing site insertions and risk propagation through the risk map, affecting the number of possible maneuvers.

As of computational demands depicted in Fig. 5, the time needed for inserting the found landing sites into the risk map scales linearly with s. The unexpected decrease in the computational time needed for risk propagation with increasing s results from accessing more compact areas in the computer memory, thus reducing access times.

Increasing the number of heading samples increases the number of nodes with possible forced landing and nodes connected to an airport. More heading samples lead to a more extensive set of plausible maneuvers Λ. Thus, increased heading resolution allows connecting more nodes in the risk map and thus lowers the risks. However, the computational demands increase with k significantly; see Fig. 5. The asymptotic complexity of the risk propagation can be bounded by $\mathcal{O}(|\Lambda|\,|Q|)$, where $|\Lambda|$ is the number of maneuvers for finding a successor node from the given node, and $|Q|$ is the number of samples of $\mathcal{C}_{\text{free}}$. Note that the instances for $k = 32, s \in [50, 75]$ have not finished within the given 23 hours; see Table I.

The most demanding part of the proposed method is connecting the selected landing sites to the risk map and consequent risk propagation. Anything else, including precomputation of Λ or selecting the landing sites, is negligible.

Once the risk map is computed, a loss of thrust-induced risk for any configuration can be queried in about 1.6 s on average. Three query locations have been selected for presenting the associated risk. For small s and k, emergency landing is unknown from q_1 and q_3, indicated as '–' in Table I. Increased k yields landing at less risky landing sites as more connections are considered. Further increase of k allows landing at the airport as the risk becomes zero for q_1.

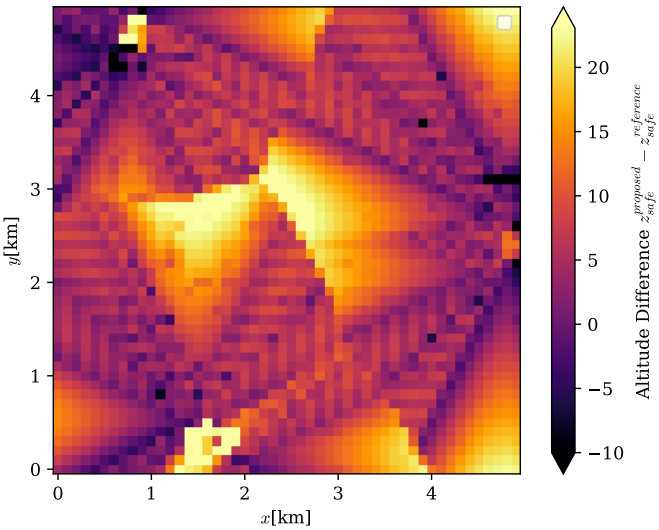

Fig. 6. Minimum safe altitude difference between the proposed method with $k = 32$ and the reference [8]. The reference method utilizes maneuvers with minimal altitude loss, leading to the optimal safe altitude map. The proposed method discretizes the configuration space, so maneuvers with greater than minimal altitude loss are planned. The found safe altitude is higher than in [8]; however, the proposed method addresses the limitation of [8] and determines the risk induced by loss of thrust even for configurations under such a safe altitude limit.

Comparision with the Former Approach

The approaches are compared using a minimum safe altitude map extracted from the proposed risk map with $k = 32$ as the altitude of the lowest nodes with zero risk. The reference method [8] has been run for 10 min and provides a safe altitude map built from a planning tree with approx. 8000 nodes. The safe altitude maps are compared as altitude difference depicted in Fig. 6.

From the altitude difference, it can be observed that the reference method provides a lower safe altitude because of the discrete uniform sampling in the proposed method. The reference method determines the smallest altitude loss possible, leading to the optimal safe altitude map. Significant altitude differences are around the airports because the discretization leads to inserting almost full turns as the configuration in the risk map and the landing sites are too close to each other; thus, a higher safe altitude is provided by the proposed method. Besides, the maneuvers in the proposed method have higher altitude loss, also due to discretization. However, in cases where the proposed method provides a lower altitude than the reference method, the same happens in the reference method. It also needs to insert an extra turn due to the sampling; however, since the reference method utilizes random sampling, the case is less occurring.

VI. Conclusion

We present a generalization of the approach [8] to address the RELP problem. The proposed method minimizes the loss of thrust-induced risk even if airports are not reachable by providing the least risky emergency landing at other-than-airport landing sites. The method is based on explicit discretization and efficient risk propagation through the risk map. A risk associated with any configuration can be queried within less than two seconds once the risk map is determined.

The proposed method has been evaluated on a realistic urban scenario, and its minimum safe altitude has been compared with the former work. Although the proposed method provides a higher minimum safe altitude than the reference method due to discretization, its main feature is evaluating the risk for configurations below that altitude. Hence, the proposed method enables risk-aware planning even in the phases of the flight when the minimum safe altitude is not reached, such as after take-off, or when the total risk considering other failures is lower without a safe emergency landing guarantee. Thus, the method is suitable for in-flight loss of thrust-induced risk evaluation for risk-aware planning scenarios in urban environments.

References

[1] S. Hasan, "Urban air mobility (uam) market study," National Aeronautics and Space Administration (NASA), Tech. Rep., 2019.

[2] M. Moore, "21st century personal air vehicle research," in *AIAA International Air and Space Symposium and Exposition: The Next 100 Years*, 2003, p. 2646.

[3] J. D. Kenny, *26th Joseph T. Nall Report*. Richard G. McSpadden, JR., 2017.

[4] Australian Transport Safety Bureau, "Engine failures and malfunctions in light aeroplanes 2009–2014," *Investigation number AR-2013-107, 9 March 2016*, pp. 1–38, 2016.

[5] X. Hu, B. Pang, F. Dai, and K. H. Low, "Risk assessment model for uav cost-effective path planning in urban environments," *IEEE Access*, vol. 8, pp. 150 162–150 173, 2020.

[6] K. Dalamagkidis, K. Valavanis, and L. Piegl, "On integrating unmanned aircraft systems into the national airspace system, international series on intelligent systems, control, and automation: Science and engineering," *Science and Engineering*, vol. 36, 2009.

[7] J. Sláma, P. Váňa, and J. Faigl, "Risk-aware trajectory planning in urban environments with safe emergency landing guarantee," in *IEEE International Conference on Automation Science and Engineering (CASE)*, 2021, pp. 1606–1612.

[8] P. Váňa, J. Sláma, J. Faigl, and P. Pačes, "Any-time trajectory planning for safe emergency landing," in *IEEE/RSJ International Conference on Intelligent Robots and Systems (IROS)*, 2018, pp. 5691–5696.

[9] H. Chitsaz and S. M. LaValle, "Time-optimal paths for a dubins airplane," in *IEEE Conference on Decision and Control*, 2007, pp. 2379–2384.

[10] L. E. Dubins, "On curves of minimal length with a constraint on average curvature, and with prescribed initial and terminal positions and tangents," *American Journal of mathematics*, vol. 79, no. 3, pp. 497–516, 1957.

[11] M. Owen, R. W. Beard, and T. W. McLain, "Implementing dubins airplane paths on fixed-wing uavs," in *Handbook of Unmanned Aerial Vehicles*. Springer, 2015, pp. 1677–1701.

[12] S. Paul, F. Hole, A. Zytek, and C. A. Varela, "Flight Trajectory Planning for Fixed-Wing Aircraft in Loss of Thrust Emergencies," *arXiv preprint arXiv:1711.00716*, 2017.

[13] S. Primatesta, A. Rizzo, and A. la Cour-Harbo, "Ground risk map for unmanned aircraft in urban environments," *Journal of Intelligent & Robotic Systems*, vol. 97, no. 3, pp. 489–509, 2020.

[14] G. Fasano, F. Causa, A. Franzone, C. Piccolo, L. Cricelli, A. Mennella, and V. Pisacane, "Path planning for aerial mobility in urban scenarios: the smartgo project," in *IEEE International Workshop on Metrology for AeroSpace (MetroAeroSpace)*, 2022, pp. 124–129.

[15] A. la Cour-Harbo, "Ground impact probability distribution for small unmanned aircraft in ballistic descent," in *International Conference on Unmanned Aircraft Systems (ICUAS)*, 2020, pp. 1442–1451.

[16] P. Eng, "Path planning, guidance and control for a uav forced landing," Ph.D. dissertation, Queensland University of Technology, 2011.

[17] P. F. A. Di Donato and E. M. Atkins, "An off-runway emergency landing aid for a small aircraft experiencing loss of thrust," in *AIAA Infotech@ Aerospace*, 2015, p. 1798.

[18] P. F. A. Di Donato, "Toward autonomous aircraft emergency landing planning," Ph.D. dissertation, University of Michigan, 2017.

[19] R. Church and C. ReVelle, "The maximal covering location problem," in *Papers of the regional science association*, vol. 32, no. 1. Springer-Verlag Berlin/Heidelberg, 1974, pp. 101–118.

[20] H. S. Amarilies, A. P. Redi, I. Mufidah, and R. Nadlifatin, "Greedy heuristics for the maximum covering location problem: A case study of optimal trashcan location in kampung cipare–tenjo–west java," in *IOP Conference Series: Materials Science and Engineering*, vol. 847, no. 1, 2020, p. 012007.

[21] X. He, C. Jiang, L. Li, and H. Blom, "A simulation study of risk-aware path planning in mitigating the third-party risk of a commercial uas operation in an urban area," *Aerospace*, vol. 9, no. 11, 2022.

[22] S. Primatesta, G. Guglieri, and A. Rizzo, "A risk-aware path planning strategy for uavs in urban environments," *Journal of Intelligent & Robotic Systems*, vol. 95, no. 2, pp. 629–643, 2019.

[23] R. Standard, "321-07, common risk criteria for national test ranges. range safety group risk committee, range commanders council," *US Army White Sands Missile Range, New Mexico*, 2007.

[24] OpenStreetMap contributors, "Planet dump retrieved from https://planet.osm.org," https://www.openstreetmap.org, 2023, accessed on: 28 Feb 2023.

[25] NASA, "Nasa shuttle radar topography mission global 1 arc second," https://opentopography.org/, 2013, accessed on: 28 Feb 2023.

[26] Facebook Connectivity Lab and Center for International Earth Science Information Network - CIESIN - Columbia University, "High Resolution Settlement Layer (HRSL). Source imagery for HRSL © 2016 DigitalGlobe," 2016, accessed on: 28 Feb 2023.

[27] J. Bezanson, A. Edelman, S. Karpinski, and V. B. Shah, "Julia: A fresh approach to numerical computing," *SIAM review*, vol. 59, no. 1, pp. 65–98, 2017.